

A New Multi-path Vector Channel Simulator for the Performance Evaluation of Antenna Array Systems

Alex Stéphenne and Benoît Champagne

INRS-Télécommunications, Université du Québec, 16 place du Commerce
Verdun, Québec, Canada H3E 1H6
email: {stephenn,bchampgn}@inrs-telecom.quebec.ca

Abstract

In this paper, we present a new, computationally efficient simulator for time-varying multi-path (fast fading) vector channel that can be used to evaluate the performance of antenna array wireless receivers. The development of the simulator is based on the emulation of the spatio-temporal correlation properties of the vector channel. The channel is modeled as a multi-channel FIR system with time-varying coefficients which are obtained via the application of a space-time correlation shaping transformation on some independent random sequences. The various parts of the new simulator are detailed and channel simulation realizations are presented and commented.

1 INTRODUCTION

Because of the limited availability of spectrum, wireless system designers are under pressure to achieve high spectral efficiency. To this end, future wireless systems will almost certainly use adaptive antenna arrays [1]. Since performance analysis of communication systems is often done first via computer simulations, there is a need for an effective multi-path vector (multi-antenna) channel simulator. The design of such a simulator must be done with great care since the performance increase associated with the use of beamforming, space diversity and/or path diversity for a given simulated system is strongly dependent on the temporal and spatial characteristics of the channel.

To study the performance of antenna array receivers via simulation, it is often assumed for simplicity that the multi-path channel parameters vary slowly as compared to the symbol duration, so that a fixed vector channel can be used (e.g. [2]-[5]). The main limitation of such an approach is that one can obviously not study the tracking properties of the algorithms used to adapt the receiver filters. Recently, a time-varying vector channel simulator has been presented in [6]. The latter decomposes the channel in its time-varying components due to each of the propagation paths, whether

they are temporally differentiable or not¹. Such a simulator becomes very computationally expensive when the number of propagation paths is large, as can be the case in a typical urban environment.

In this paper, we present a new computationally efficient simulator for time-varying multi-path (fast-fading) vector channels that can be used to evaluate the performance of antenna array wireless receivers. The development of the simulator is based on the emulation of the spatio-temporal correlation properties of the channel. The channel is modeled as a multi-channel FIR system with time-varying channel coefficients which are obtained via the application of a space-time correlation shaping transformation on some independent random sequences. The new simulator is a multi-channel generalization of the scalar channel presented in [7]. The main advantage of the new simulator, as opposed to the one presented in [6], is that its computational complexity is now proportional to the number of time-differentiable paths, regardless of the number of indifferently differentiable ones. Another advantage is that fewer topographical parameters are being feed into the simulator making it less environment dependent.

2 THE MULTI-PATH VECTOR CHANNEL

In this section we present the multi-path wireless vector channel model used in the development of the simulator.

2.1 Transmission Model

We consider the transmission of a signal from a mobile (single antenna) to a base (multiple antennas), i.e. the uplink transmission. We suppose that the mobile is surrounded by local reflecting structures so that there is no line of sight between the mobile and the base. In order to present the channel model, the following relevant parameters are defined:

¹In order for two paths to be time-differentiable, their relative delay of arrival must be greater than the inverse of the bandwidth of the transmitted signal.

- f_c , the carrier frequency ($\omega_c = 2\pi f_c$);
- c , the speed of light;
- λ_c , the carrier wavelength;
- B , the transmitted signal bandwidth;
- v , the speed of the mobile;
- N_e , the number of antenna in the array;
- D the array dimension;
- τ_{min} and τ_{max} , the minimum and maximum propagation delay from the mobile to the base (multi-path) ($\tau_{max} = \tau_{min} + \text{delay spread}$).

We assume that $D \ll c/B$ (narrowband array assumption). This assumption is respected for many wireless communication systems. As an example, consider IS-95 for which $B = 1.25\text{MHz}$, the assumption tells us that $D \ll 240\text{m}$. Under this assumption, it can be shown that the baseband equivalent of the N_e -dimensional vector channel impulse response is given by

$$\mathbf{g}(t, u) = \sum_{i=0}^{M-1} \delta(t - u - \tau_i) \mathbf{a}_i(\omega_c, t). \quad (1)$$

where t is the observation time, u is the time at which the impulse $\delta(\cdot)$ is applied, M is the number of time-differentiable paths, τ_i is the propagation delay for the i^{th} path and $\mathbf{a}_i(\omega_c, t)$ is called here the i^{th} complex path vector. This result is similar to results derived in the literature [6, 4]. The new simulator generates the complex path vectors which has for elements the channel coefficients. Those coefficients are functions of time and frequency.

In a typical urban or suburban environment, all time-differentiable paths are composed of a large number of time-indifferentiable subpaths. By the central limit theorem we therefore find the channel coefficients to be well approximated by complex Gaussian variables (Rayleigh envelope) [8]. Since Gaussian variables are entirely characterized by their first and second order statistics, we can simulate the channel simulator coefficients by generating Gaussian variables that have some predefined appropriate first and second order statistics (mean and correlation). It is easily shown that the channel coefficients are zero-mean [8]. In the next section we develop a closed form expression for the second order statistics of the channel coefficients.

2.2 Second Order Characterization

Since we suppose that the mobile is surrounded by local reflecting structures, we have a lot of indirect transmission subpaths each of which exhibiting different properties. With such a scenario, it is reasonable to use the following hypotheses:

1. The i^{th} ($i = 0, \dots, M-1$) differentiable path is composed of an infinite number of subpaths with delays ranging from $\tau_{min} + 1/B$ to $\tau_{min} + (i+1)/B$.
2. The Doppler angle is uniformly distributed in $[0, 2\pi]$.
3. Subpaths corresponding to different delays, angles of arrival or Doppler angles have uncorrelated amplitudes.
4. For a given subpath, the delay, angles of arrival and Doppler angle are mutually independent.

Also, to simplify the analysis, we assume that $v\tau_{max} \ll \lambda_c$. This assumption is always respected in vehicular technology ($v < 30\text{m/s}$, $\tau_{max} < 50\mu\text{s}$) provided $f_c \ll 200\text{GHz}$. Under these hypotheses one may show that the cross-correlation matrix of the path vectors is given by (similar result in [4])

$$\begin{aligned} \mathbf{R}_{ij}(\omega_c, t_1, t_2) &\triangleq E[\mathbf{a}_i(\omega_c, t_1) \mathbf{a}_j^H(\omega_c, t_2)], \quad (2) \\ &= \delta_{ij} J_0(\omega_d \Delta t) F_a(i) \mathbf{R}_{\mathbf{v}_i}(\omega_c) \quad (3) \end{aligned}$$

where: $\omega_d = \omega_c v/c$ is the radial Doppler frequency; $\Delta t = |t_2 - t_1|$, $J_0(\cdot)$ is the Bessel function of the first kind and of order 0; $F_a(i)$ is the integral of the density function of the transmission delay over the interval that corresponds to the i^{th} path; and the matrix $\mathbf{R}_{\mathbf{v}_i}(\omega_c)$ is given by

$$\mathbf{R}_{\mathbf{v}_i}(\omega_c) = \int_0^{2\pi} \int_{-\pi/2}^{\pi/2} f_c(\theta, \xi) \mathbf{v}_i(\omega_c, \theta, \xi) \mathbf{v}_i^H(\omega_c, \theta, \xi) d\theta d\xi. \quad (4)$$

In (4),

$$\mathbf{v}_i = [1, e^{-j\omega_c \rho_{1i}}, \dots, e^{-j\omega_c \rho_{N_e-1,i}}]^T, \quad (5)$$

is the steering vector of the array, $f_c(\theta, \xi)$ is the joint density function of angles of arrival θ (azimuth angle) and ξ (elevation angle), and ρ_{ji} is the time difference of arrival (relative to antenna 0) for the i^{th} path on the j^{th} antenna.

Typically, a negative exponential distribution is used to describe the density function of the transmission delays [9], so that one finds

$$F_a(i) = \left[1 - e^{-1/(B\bar{T})}\right] e^{-i/(B\bar{T})} \quad (6)$$

where \bar{T} is the mean delay. The cross-correlation matrix of the path vectors, $\mathbf{R}_{\mathbf{v}_i}(\omega_c)$, can be obtained from (4) once the speed of the mobile v , the antenna geometry (or equivalently the function $\rho_{ji}(\theta, \xi)$ in (5)), and the path angles of arrival distribution $f_c(\theta, \xi)$ are given.

3 SIMULATOR STRUCTURE

The basic philosophy behind the new simulator is to devise some kind of space-time correlation shaping transformation that will be applied to uncorrelated Gaussian white noise sequences in order to obtain time-varying path vectors $\mathbf{a}_i(\omega_c, t)$ ($i = 0, \dots, M-1$) exhibiting the appropriate spatio-temporal correlation properties, as given by (3). Such a transformation would provide a

multi-channel generalization of the scalar channel simulator presented in [7].

Observation of (3) indicates that the path vectors are independent, which means that the channel coefficients can be generated independently for each differentiable path by the simulator. Furthermore, by rewriting (3) in the following way for the case $i = j$:

$$\mathbf{R}_{ii}(\omega_c, \Delta t) = J_0(\omega_d \Delta t) \mathbf{C}_i(\omega_c) \quad (7)$$

where

$$\mathbf{C}_i(\omega_c) = F_a(i) \mathbf{R}_{v_i}(\omega_c), \quad (8)$$

we can see that in order to obtain the appropriate space-time correlation characteristics for a given path, one can use a time transformation followed by a spatial transformation. Note that from now on, since for a given system the carrier frequency is usually fixed, we will omit to indicate ω_c dependencies. A time-correlation shaping filter need to be devised for the temporal component of the correlation, namely $(J_0(\omega_d \Delta t))$. A linear time invariant discrete-time filter is used and its impulse response is denoted by $h(m)$. Note that the same filter will be used for each path since the time correlation part is independent of the index i . A separated transformation also need to be devised for the spatial component of the correlation, i.e. \mathbf{C}_i in (8). This transformation will be applied on a vector formed by taking the output of the time shaping filters (multiple antennas) at a given time. From now on we simply refer to this vector as the spatially uncorrelated signal vector \mathbf{y} .

The sampling rate for $h(m)$ must be high enough to permit the use of simple interpolation procedures later on, at the channel simulator output, when a higher sampling rate is required. We took the sampling interval T equal to $2\pi/(3\omega_d)$ which is more than adequate since it corresponds to $3/2$ the Nyquist rate ($1/T = 3/2 \times 2f_d$). A method based on the minimization of a quadratic error on the power spectral density was developed to design a causal and stable pole-zero filter $h(m)$, whose z -transform is denoted by $H(z)$. The exact expression for the obtained time-correlation shaping filter $H(z)$ is

$$H(z) = \frac{0.717 + 1.705z^{-1} + 2.251z^{-2} + 1.513z^{-3} + 0.536z^{-4}}{1 + 1.743z^{-1} + 2.334z^{-2} + 1.343z^{-3} + 0.596z^{-4}}. \quad (9)$$

Fig. 1 illustrates the desired temporal correlation, $J_0(2/3\pi m)$, as well as the temporal correlation of a discrete-time signal obtained by passing a white noise sequence through the filter $H(z)$ given in (9).

The development of the transformation used to obtain the spatial component of the correlation is based on the Karhunen-Loève expansion of \mathbf{C}_i in (8). Denote by \mathbf{Q}_i the matrix whose columns are the orthonormalized eigenvectors of \mathbf{C}_i and by $\mathbf{\Lambda}$ the diagonal matrix which entries are the corresponding eigenvalues λ_{ij} ($j = 0, \dots, N_e - 1$). Premultiplication of the spatially

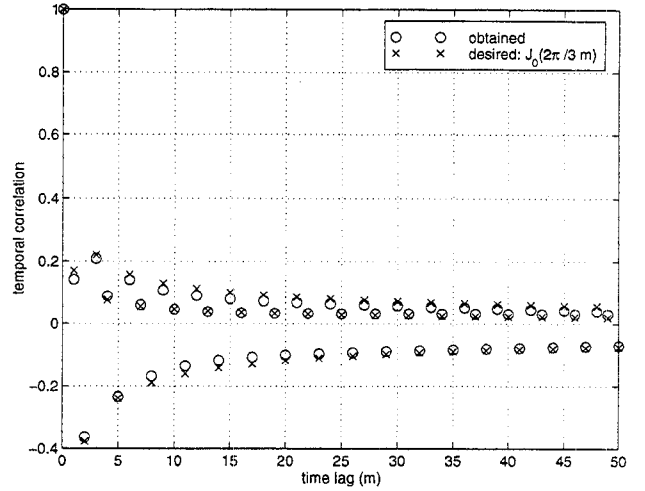


Figure 1: Desired and obtained temporal correlations.

uncorrelated signal vector \mathbf{y}_i by $\mathbf{Q}_i \mathbf{\Lambda}^{1/2}$ gives a vector with the required spatial correlation properties.

By combining the time-correlation shaping filter and the spatial transformation, we end up with a procedure for synthesizing random vectors with the desired space-time correlation properties. For each time-differentiable path of interest, the structure shown in Fig. 2 is used to obtain the simulated time-varying path vectors $\tilde{\mathbf{a}}_i(m)$ ($i = 0, \dots, M - 1$), where the time index m refers to the update rate of the path vectors. In this figure, the $\tilde{n}_{ij}(m)$ ($j = 0, \dots, N_e - 1$) are uncorrelated complex Gaussian white noise sequences with zero mean. These sequences are fed to the time-correlation shaping filter denoted by $H(z)$, the output of which are the elements of the spatially uncorrelated signal vector \mathbf{y}_i denoted by y_{ij} . The y_{ij} are scaled by the eigenvalues λ_{ij} and are then passed through the spatial transformation \mathbf{Q}_i . The result is the elements of the simulated i^{th} path vector $\tilde{\mathbf{a}}_i(m)$. Finally, the path vectors obtained from Fig. 2 are interpolated at the sampling rate of the discretized transmitted signal which we take equal to the bandwidth of the transmitted signal, B . The time index after interpolation is denoted by the letter k , and the corresponding sampling interval by $T_c = 1/B$.

The final channel simulator is shown in Fig. 3. The input to the channel simulator, $z(k)$, is the baseband transmitted signal, the outputs, $s_j(k)$ ($j = 0, \dots, N_e - 1$) are the baseband received signal at the N_e antennas. The simulator is based on a tapped-delay-line model, with evenly spaced taps T_c apart. Each tap output is multiplied by a time-varying coefficient $\tilde{a}_{ij}(k)$ which is the j^{th} element of the i^{th} simulated path vector obtained with the structure of Fig. 2. A complex noise signal $n_j(k)$ modeling any external noise is added to the tapped delay line output. The standard deviation σ of that noise is chosen according to the required SNR.

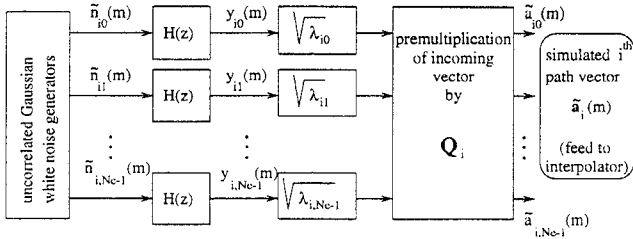


Figure 2: Structure of the path vector generator (one such structure for each time-differentiable path i).

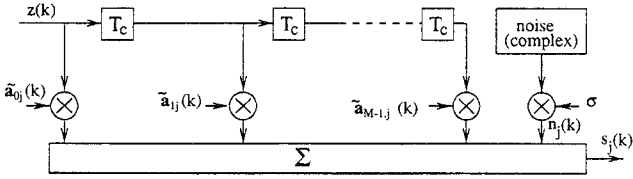


Figure 3: Time-varying vector channel simulator (one such structure for each antenna j).

4 SIMULATION EXAMPLE

In this section we present and analyze a channel realization obtained with the new time-varying vector channel simulator described above.

In this example, we consider $M = 3$ time-differentiable paths and $N_e = 7$ receiving antennas uniformly distributed around a horizontal circular array and separated by half a wavelength. To simplify the analysis of the directivity of the channel we assume that all the propagation paths lie in the same plane as the array (elevation angle $\psi = 0$), and that they are uniformly distributed in azimuth angle in $\theta_i \pm \Delta_i$, where θ_i is the mean angle of arrival and $2\Delta_i$ is the angle spread for the i^{th} path. In our example, $\theta_0 = 90^\circ$, $\theta_1 = 150^\circ$, $\theta_2 = 270^\circ$, $\Delta_0 = 2.5^\circ$, $\Delta_1 = 5^\circ$ and $\Delta_2 = 1^\circ$. These parameters are displayed in table 1 for quick reference. The speed of the mobile is taken to be $30m/s$ ($108km/h$), the carrier frequency f_c is $1GHz$ (Doppler frequency $f_d = 100Hz$), the transmitted signal bandwidth B is $1.25MHz$, the mean delay \bar{T} in (6) is set to $2/B = 2T_c$, and the channel is updated once every $4096T_c$ before the interpolation which bring the update rate to once every T_c .

Fig. 7 illustrates the evolution in time of the magnitude of the channel coefficients for antenna 0, $\tilde{a}_{i0}(k)$ ($i = 0, 1, 2$). The sum of those magnitudes is also shown to exemplify what can be achieved via path diversity when the paths are coherently combined. Comparing the shapes of the curves in Fig. 7 with what is shown in the literature (in [11] for example), we see that the time evolution of the simulated channel coefficients is representative of a typical wireless channel.

Next, we show that the spatial characteristics of the simulated channel coefficients are also representative of a typical wireless channel. To this end, we look at the directivity patterns of a receiver matched to the simulated

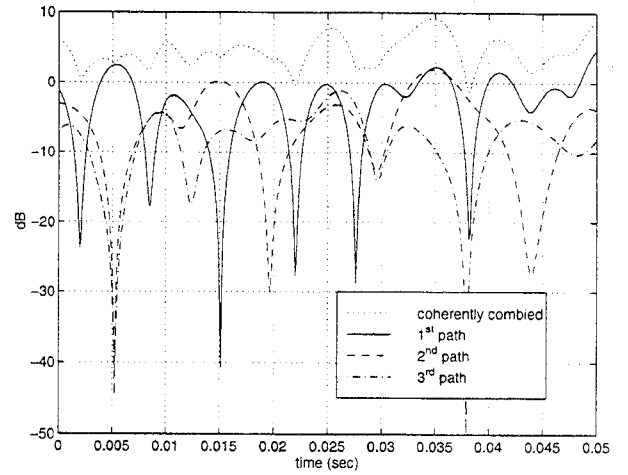


Figure 4: Channel coefficient magnitudes vs time for antenna 0.

channel. The directivity pattern is simply a graph of the gain of the receiver vs the azimuth angle θ (and frequency if the frequency is not set to a particular value) of the incoming paths. The directivity pattern at time $t = 0$ for all possible values of normalized frequency and azimuth angle is shown in Fig. 4. We can see that, as expected, most of the incoming energy arrives at azimuth angles near θ_i , $i = 0, 1, 2$ as given above.

In order to visualize the spatial directivity, the normalized frequency is set to 0 (i.e. carrier frequency for passband equivalent channel) for the remaining figures. Fig. 5 illustrates the variation in time of the directivity pattern (linear scale), while the directivity patterns (in dB) for two specific values of time, $t = 15ms$ and $50ms$, are given in Fig. 6. We can clearly see that much of the incident energy arrives from around the mean azimuth angles θ_i , $i = 0, 1, 2$. Furthermore, by comparing Fig. 5 and 6 to Fig. 7, we see that the directivity pattern gain for azimuth angles near θ_i follows closely the magnitude of the channel coefficients $\tilde{a}_{i0}(k)$. Note that there is not a perfect match between the maxima of the directivity patterns and the mean azimuth angles θ_i , $i = 0, 1, 2$. This is due to the fact that there is a trade-off between the effects of beamforming and spatial diversity because of the imperfect fading correlation between the antennas.

The observations presented in this section and others made on similar channel realizations obtained for different simulation scenarios lead us to the conclusion that the new simulator is an attractive working alternative to existing vector channel simulator. The new simulator is easy to use and models realistic channel behavior while having a complexity proportional to the number of time-differentiable paths, regardless of the number of indifferentiable ones.

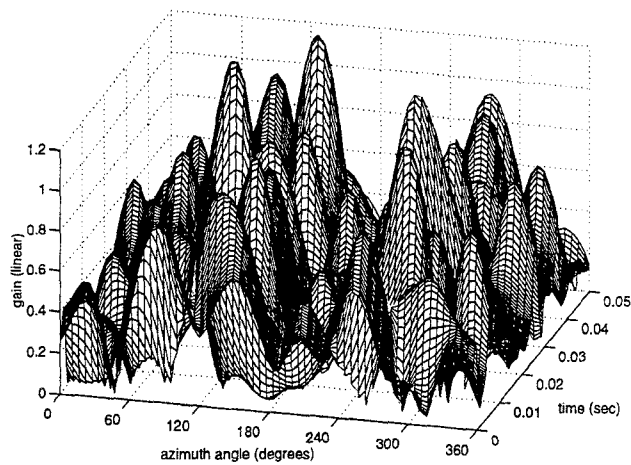


Figure 6: Directivity pattern (linear) at carrier frequency vs time for receiver matched to simulated channel.

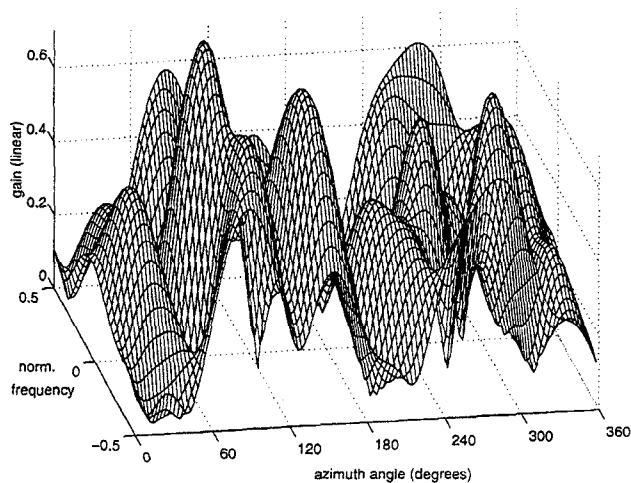


Figure 5: Directivity pattern (linear) for receiver matched to simulated channel at $t = 0$.

	$i = 0$	$i = 1$	$i = 2$
mean angle, θ_i (degrees)	90	150	270
angle spread, $2\Delta_i$ (degrees)	5	10	2

Table 1: Path angle of arrival parameters.

References

[1] D. B. Woerner, J. H. Jeffrey and T. S. Rappaport, "Simulation issues for future wireless modems," *IEEE Commun. Magazine*, pp. 42–53, July 1994.

[2] B. H. Khalaj, A. Paulraj and T. Kailath, "2D RAKE receivers for CDMA cellular systems," *Proceedings of IEEE Global Communications Conference*, San Fransisco, CA, pp. 1–5, Dec. 1994.

[3] R. Kohno, P. B. Rapajic and B. S. Vucetic, "An overview of adaptive techniques for interference

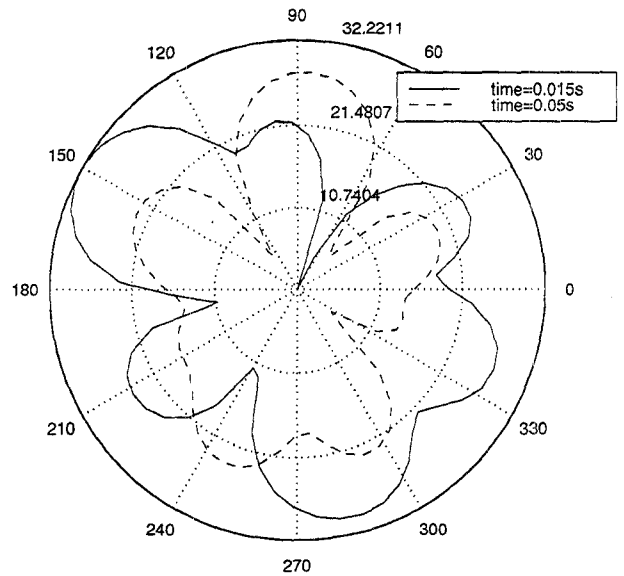


Figure 7: Directivity pattern (dB) at carrier frequency for receiver matched to simulated channel for two different values of time ($t = 15ms$ and $t = 50ms$).

minimization in CDMA systems," *Wireless Personal Commun.*, Kluwer, pp. 3–21, 1994.

- [4] A. F. Naguib, A. Paulraj, "Performance of DS/CDMA with M-ary orthogonal modulation cell site antenna arrays," *Proc. ICC'95*, Seattle, WA, USA, pp. 697–702, June 1995.
- [5] M. Nagatsuka and R. Kohno, "A spatially and temporally optimal multi-user receiver using an array antenna for DS/CDMA," *IEICE Trans. Commun.*, vol. E78-B, no. 11, pp. 1489–1497, Nov. 1995.
- [6] G. Rayleigh, S. N. Diggavi, A. F. Naguib and A. Paulraj, "Characterization of fast fading vector channels for multi-antenna communication systems," *Proc. 28th Asilomar Conf. on Signal, Systems and Computers*, pp. 853–857, Nov. 1995.
- [7] G. J. R. Povey, P. M. Grant and R. D. Pringle, "A Decision-Directed Spread-Spectrum RAKE Receiver for Fast-Fading Mobile Channels," *IEEE trans. on vehicular technology*, vol. 45, no. 3, Nov. 1996.
- [8] A. F. Naguib, "Adaptive antennas for CDMA wireless network," Ph.D. Thesis, Stanford Univ., 1996.
- [9] M. D. Yacoub, *Foundations of Mobile Radio Engineering*, CRC Press, 1993.
- [10] A. V. Oppenheim and R. W. Schaffer, "Digital Signal Processing," 1st edition, Prentice-Hall, 1975.
- [11] A. Paulraj, "Diversity Techniques," in *The Mobile Communications Handbook*, J. D. Gibson, Ed., CRC Press, Florida, pp. 166–176, 1996.